Mapping Land Cover Types using Sentinel-2 Imagery: A Case Study

Laura Annovazzi-Lodi, Marica Franzini and Vittorio Casella
Department of Civil Engineering and Architecture, University of Pavia, Via Ferrata 5, Pavia, Italy

Keywords: Sentinel-2, Remote Sensing, Supervised Classification, SVM and Land Cover.

Abstract: This paper presents a case study of automatic classification of the remotely sensed Sentinel-2 imagery, from the EU Copernicus program. The work involved a study site, located in the area next to the city of Pavia, Italy, including fields cultivated by three farms. The aim of this work was to evaluate the so-called supervised classification applied to satellite images and performed with Esri's ArcGIS Pro software and Machine Learning techniques. The classification performed produces a land use map that is able to discriminate between different land cover types. By applying the Support Vector Machine (SVM) algorithm, it was found that, in our case, the pixel-based method offers a better overall performance than the object-based, unless a specific class is exclusively taken into consideration. This activity represents the first step of a project that fits into the context of Precision Agriculture, a recent and rapidly developing research area, whose aim is to optimize traditional cultivation methods.

1 INTRODUCTION

The World Population Prospect document of the United Nations (DESA, 2017) predicts that the world population will rise to 9.8 billion by 2050. All over the planet, there will be a corresponding increment in food demand, and this is one of the major humanity challenges.

Furthermore, climate change, environmental degradation, the ever increasing demand for water and energy, socio-political and economic changes are just a few examples of factors that necessarily motivate us to integrate technological innovation in the productive processes of modern agriculture in a consolidated way that makes it more fruitful and, at the same time, sustainable (MiPAAF, 2017), (Chhetri et al., 2012).

Thematic maps show the spatial distribution of a generic indicator and depict environmental and physical factors (geological maps, distribution of water resources, entity of precipitations, etc.), biological (distribution of forests, surface of agricultural crops and their production, etc.) or social ones (census distribution, population's average age, health, etc.). Land use maps are particular thematic maps where the terrain is subdivided into several categories belonging to a pre-defined list such as: roads, buildings, forest, fields and so on: the level of detail of the classification depends on the goal and on the degree of detail of the data used to produce the map.

The most used way to produce large-scale land use maps is the classification of remote sensing images.

Among land cover maps, crop type maps are necessary for different purposes and provide crucial information for monitoring and management of the agricultural sector. According to (Marais-Sicre et al., 2016) they can be employed, for example, to estimate the specific use of water for a certain type of cultivation or to identify the various types of crops before the start of the irrigation season, so as to study the best strategy resource management for water, which is both sustainable and resourceful. They are also useful in creating growth models that allow for estimation of crop yield.

These maps are therefore essential in the field of Precision Agriculture (PA). PA is the application of technologies and principles to manage spatial and temporal variability associated with all aspects of agricultural production for improving crop performance and environmental quality (Pierce and Nowak, 1999). PA is based on a bunch of Geomatics techniques: territory survey, satellite navigation and GIS. Crop maps are also required by policy and decision-makers for economics, management and for agricultural statistics (Immitzer et al., 2016). Information recorded and produced in the frame of PA could facilitate different administrative and control procedures (Zarco-Tejada et al., 2014).

Annovazzi-Lodi, L., Franzini, M. and Casella, V.
Mapping Land Cover Types using Sentinel-2 Imagery: A Case Study.
DOI: 10.5220/0007738902420249
In *Proceedings of the 5th International Conference on Geographical Information Systems Theory, Applications and Management (GISTAM 2019)*, pages 242-249
ISBN: 978-989-758-371-1

The goal of this study is to assess supervised classification, both object- and pixel-based, applied to a Sentinel-2 image. This activity is the first step of a project of classification of parcels of land according to the type of agricultural crop practiced, that fits into the context of PA.

2 MATERIALS

2.1 Study Area

The study site (Figure 1) is located about 15 km northwest of the city of Pavia, Italy; it covers a total area of 3220 ha. The considered site belongs to the territory of the Pianura Padana, which offers the best conditions for the cultivation of rice: wet climate, loose soil and large water availability. The study area contains different land covers/use categories such as cropland, woods, industrial and urban areas, roads and a stretch of the river Ticino including its meanders.

2.2 Ground Truth

By interviewing farm owners, in situ reference data concerning the year 2017, was collected. The information gathered for each agricultural plot was crop type, sowing and harvesting date. The plots are characterized by a large variety of shapes (square, rectangular or triangular). The main cultivated crops in this region are ryegrass, maize, barley, grassland, rice, rye and soybean.

The reference data concerning the rest of the site, such as the water of the river Ticino or the asphalt of the roads, was obtained observing a very high-resolution satellite image, acquired by Digital Globe and provided by Esri within its products; its ground resolution is, for the considered area, 30 cm. The so-obtained data was also verified both by examining the relative Google Street View images and by direct inspection of the areas under study.

Based on the data collected and observed, 439 polygons were manually drawn and created, corresponding to a total area of just over 800 ha. To precisely draw the polygons, the raster maps of the fundamental regional cartography were downloaded from the Geoportal of the Lombardy Region (URL-1), related to the area of interest. Since the regional maps are not completely up-to-date, and are therefore considered only partially reliable, the high-resolution satellite image mentioned above was jointly used as base map.

It was decided to eliminate polygons exclusively dedicated to rye, soybean, pea and other vegetables (and not the plots intended for catch crop cultivation) because the number of polygons was not sufficient to create a distinction of the spectral signature, as well as to avoid large class imbalances. Hence, the final number of polygons taken into consideration for our study was 418, with a total area of almost 774 ha (Table 1).

The so-obtained ground truth map is organized as a time-dependent GIS layer. The record associated with each polygon has a textual field describing the time frame of the various crops related to it. Once a date is chosen, a truth map containing the real classification at that time can be defined by manually filling a numeric field.

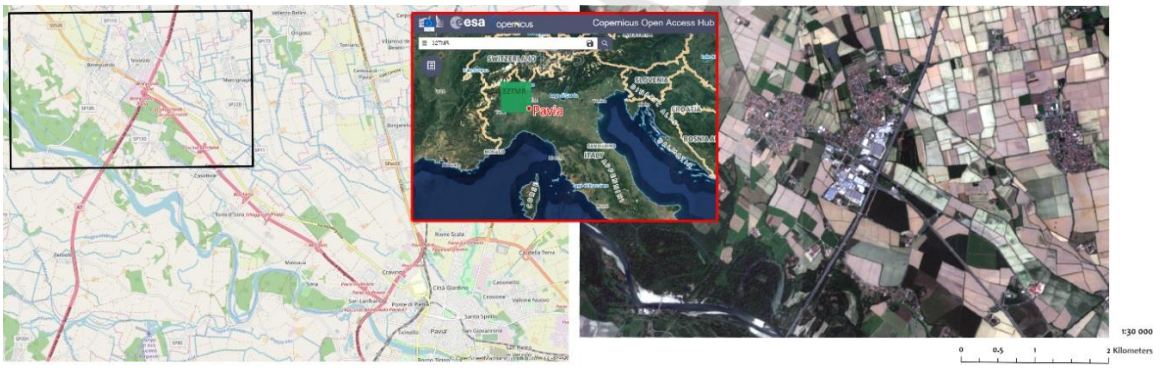

Figure 1: On the left: the study area (framed in black), next to the city of Pavia [Open Street Map]. In the middle: the extent of the Sentinel-2 Tile 32TMR (https://scihub.copernicus.eu/dhus/#/home). On the right: S-2 scene (TCI) of the study area.

Table 1: Number of polygons and surface corresponding to each class.

Class	Number of polygons	(ha)
Water	27	16.47
Asphalt	39	8.92
Wood	37	111.63
Industrial	10	15.85
Barley	25	39.12
Grassland	62	85.44
Bare soil	199	427.56
Urban	19	68.48
TOT.	418	773.47

2.3 Satellite Data and Crop Phenology

Sentinel-2 mission is a land monitoring constellation of two satellites (Sentinel-2A and Sentinel-2B, respectively launched on 22.06.2015 and on 7.03.2017) flying in the same orbit but phased at 180°, designed to give a high revisit frequency of 5 days at the Equator. It carries an innovative wide-swath, high-resolution, multi-spectral imager (MSI) with 13 spectral bands with 10, 20 and 60 m spatial resolution.

In this study, since the data collected was relative to the year 2017, all the S-2 images of that year were downloaded (concerning the area of interest, corresponding to the tile 32TMR - ESA's scene naming convention). After visual inspection, it was decided to exclude the images with high cloud coverage at the granule level and with cloud cover concentrated right in the study area. Therefore, 15 images (out of 109) were taken into consideration. Eventually, the image acquired on May 17 was chosen. The choice was considered optimal for our classification and was defined after careful considerations of several aspects listed below.

For the differentiation of crop types, phenology is considered as a key factor.

Phenology is defined as the periodicity of key events in the life cycle of living species, their chronology and their relationship between climate factors and seasonal events over time (Schwartz, 2003). For this reason, a chronogram was created, ranging from March to November and related to the major crop types (Figure 2).

During the interviews, it was possible to collect information on the timing of the vegetation cycles and the phenology of the agricultural crops that are present in the study area. The so-obtained knowledge base has been further implemented by materials found on the internet and on common agricultural books.

Ryegrass is an autumn-winter forage crop that grows rapidly. It is sown from the end of September to the beginning of November, while the harvest usually takes place in April. This plant is suitable for rotation with maize, with which it is replaced from May until mid-June.

Maize is one of the most important and widespread cereal crops in our country. Since it requires a warm and temperate climate, to facilitate its growth at ever-mild temperatures, sowing usually takes place from the end of March to April-May, but may continue until mid-June. The emergency phase can occur up to about 20 days later. Harvest takes place from the beginning of August to October.

Grassland is a stable lawn whose phenology depends on certain factors such as climatic conditions, type of soil and use (hayfields, grazed grassland or water meadow).

The water meadow is a land permanently irrigated in winter months by a veil of water, which flows by gravity in order to prevent the excessive cooling of the ground. Such a technique allows the grass to grow even at low temperatures. The water is kept moving by the slight slope of the ground. During the summer season, however, periodic irrigations of the area are carried out, as in a common lawn. In the area of the river Ticino, given the particular conformation of humps and valleys typical of these dedicated fields, the cultivation of water meadows is difficult, but for its historical importance, about 300 hectares have been preserved.

Phase	March		April		May		June		July		August		September		October		November	
	1|15	16|31	1|15	16|30	1|15	16|31	1|15	16|30	1|15	16|31	1|15	16|31	1|15	16|30	1|15	16|31	1|15	16|30
Sowing														Ryegrass	Ryegrass		Ryegrass	
		Maize	Maize		Maize		Maize											
																Barley	Barley	
				Rice	Rice													
							Soybean		Soybean									
Harvest			Ryegrass															
											Maize		Maize		Maize			
						Barley	Barley											
													Rice		Rice			
															Soybean			

Figure 2: Chronogram of sowing and harvesting periods of crops belonging to the largest number of polygons.

Barley is an unripe crop and the calendar of its vegetation cycle is rather short, giving it an excellent adaptability to very different environments. The varieties used in the study area have a good resistance to cold, so barley is sown between the end of October and early November. The harvesting phase takes place at the beginning of summer. Coming to rice, its sowing season is from April to May. In September, when the plant has reached full ripeness, the harvest begins, which lasts until October.

Based on the reported considerations, the autumn-winter dates have been excluded because almost all polygons belong to the "bare soil" category, leading to poorly significant results. May 17th was chosen because the existing crops are well defined. Indeed, mid-May is the sowing period of maize and rice crops, so their related plots are still identifiable as “bare soil”. Barley, on the other hand, is ready to be harvested, so well developed and distinguishable. Even grassland, sown in April, is lush and flourishing.

In conclusion, eight categories were considered for the described classification experiment. They are listed in Table 1 and include as agricultural crops: barley, permanent grass and wood. Also, the ground truth map was defined according to the general schedule described by the farmers; but real activities (shown in the image) can be slightly misaligned, therefore the map was tuned by observing the selected Sentinel-2 image; the adopted map is shown in Fig. 3.

3 METHODS

Different processes were applied to the collected data, by using the ESRI ArcGIS Pro software program, in order to create the land cover map. The workflow is summarized below (Figure 4):

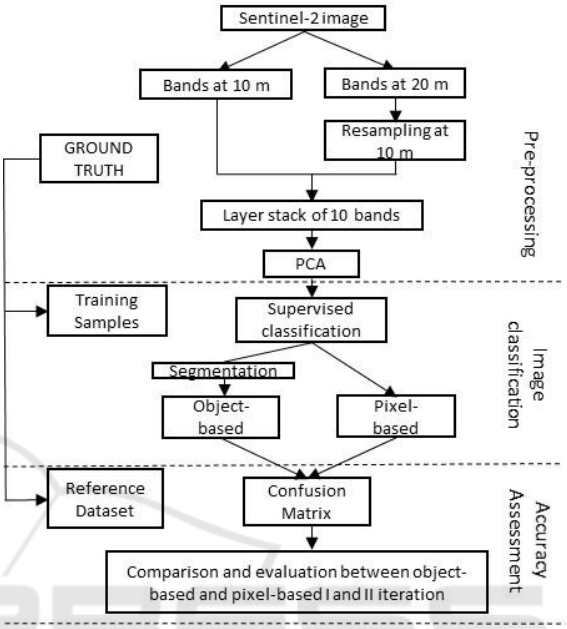

Figure 4: Workflow of our study.

Figure 3: Ground Truth corresponding to 17 May 2017. The background image is the S-2 scene (TCI) of the study area.

3.1 Pre-processing

Firstly, it should be noted that each S-2 tile covers an area of 100 km x 100 km. With the aim to alleviate the load of data during the processing stages of classification, the tile was clipped in order to circumscribe only the area of interest for our study. Atmospheric correction was not necessary because the image was clear within the study site: cloud-free Level 1 image (ToA reflectance) was used. Thanks to the flat terrain and the good geolocation accuracy, geometric pre-processing was not needed either.

For this study, it was decided to exclude the three atmospheric bands at 60 m, i.e. B1 Coastal Aerosol, B9 Water Vapor and B10 SWIR Cirrus. The four spectral bands B2 Blue, B3 Green, B4 Red and B8 NIR have a resolution of 10 m. The remaining six bands acquired at 20 m, i.e. the three of Red Edge such as B5, B6 and B7 and B8A Narrow NIR, and the two of SWIR such as B11 and B12, have been resampled. This was done in order to obtain a layer stack of 10 spectral bands at 10 m. After being resampled, each band layer has been equalized. Indeed, pixel values in each band layer were linearly stretched to the [0, 65535] interval, to give each layer the same weight, being classification sensitive to the range of gray levels.

The next step in the workflow was to apply the Principal Component Analysis (PCA). This is a mathematical method used in multivariate statistics to convert a set of variables that are probably correlated to a set of independent variables, called principal components, by using a linear transformation (Abdi and Williams, 2010). All the principal components are linear combinations of the original variables and are orthogonal to each other and therefore independent. The newly-generated components are sorted so that most of the information is mainly concentrated in the first few bands. In our case, the first three components, containing more than 99% of the original information, were only kept. It should also be noted that the first component itself contains 95% (Table 2).

Table 2: Results of the PCA step.

PERCENT AND ACCUMULATIVE EIGENVALUES			
PC Layer	Eigen Value	Percent of Eigen Values	Accumulative of Eigen Values
1	15545565733,63619	95,1596	95,1596
2	431399292,54862	2,6407	97,8003
3	300945980,90906	1,8422	99,6425
4	48264348,94573	0,2954	99,9379
5	4919188,92151	0,0301	99,9680
6	2071351,24574	0,0127	99,9807
7	1343666,65108	0,0082	99,9889
8	1082935,84931	0,0066	99,9956
9	425339,96901	0,0026	99,9982
10	297827,18188	0,0018	100,0000

In the present work, pixel-based classification is tackled, as well as object-based. The latter implies that image is segmented: adjacent pixels with similar spectral bands are grouped. Then segments are treated as a whole and classified.

ArcGIS adopts the mean shift algorithm that is a non-parametric, feature-space analysis technique for locating the maxima of a density function (Fukunaga and Hostetler, 1975), (Comaniciu and Meer, 2002). The software requires three parameters: spectral detail, spatial detail and minimum segment size. The first one sets the level of importance given to spectral differences between pixels. The second parameter controls the level of relevance given to the proximity between pixels. The last one represents a merging criterion. It is good practice to test different combinations of the parameters until the desired result is found.

Based on our experience and after visually evaluating the result of segmentation, the final parameters chosen are shown in Table 3.

Table 3: Parameters sets for the segmentation.

Spectral detail	Spatial detail	Minimum segment size in pixels
19	2	20

3.2 Classification

In general, the main objective of supervised techniques (adopted in the present work) is to learn from a training data set and to be able to make predictions, i.e. give unclassified pixels or segment a label. Ground Truth datasets are typically split into two distinct group and intended for two different functions:

-*Training samples*: once selected and labeled, they are used to train the algorithm and to generate a classification scheme, based on spectral signatures to be applied to the rest of the objects/ pixels with unknown labels;

-*Test set* (or Reference dataset): such samples are not used for training and, being labelled, can be used to assess the accuracy of classification, in a statistically independent and rigorous way.

Indeed, a supervised classification consists of three phases. The first (learning or calibration phase) and the second (prediction phase) employ training samples, instead the last one (validation phase) uses test sets. We used 50% of Ground Truth for training and 50% for validation.

A number of algorithms for supervised classification have been developed over time. We selected the multiclass Support Vector Machine (SVM) because it provides a powerful, robust and modern method. The

principal advantage of this machine-learning algorithm is that it can successfully work with a small number of training samples (Taskin et al., 2011), as in our case. Developed by Vapnik and his collaborators, instead of estimating the probability densities of the classes, it directly solves the problem of interest by determining the classification boundaries between the classes (Vapnik, 1979). Basically, the algorithm tries to find optimal hyperplanes to separate training samples into a predefined number of classes and by maximizing the margin between the classes, looking for hyperplanes as distant as possible from the training samples of classes (Kowalczyk, 2017). It is also able to separate non-linear problems through the so-called SVM trick, based on the kernel method.

3.3 Accuracy Assessment

Without a validation phase, the final classified map cannot be reliably used and, therefore, its applicability is limited. The accuracy of the classified image is assessed by comparing the classified map, obtained from the classification process, with the reference dataset. It should be noted that, usually, validation does not occur by verifying all the pixels contained in the test set, but only a limited number. We decided to randomly generate 5000 points from the test set of polygons and compare the prediction and ground truth with them. The validation phase provides information on the product quality and identifies probable sources of error by analyzing the confusion matrix, which summarizes the correct and incorrect predictions made. For pixel- and object-based classifications, the information contained in the confusion matrix is used to evaluate some common statistical measures, which express the quality of the classification. These included the overall accuracy (OA), the producer's accuracy (PA), the user's accuracy (UA), the omission and the commission errors, and the Kappa coefficient.

4 RESULTS AND DISCUSSION

In this section, classification results and accuracy assessment are shown. As already introduced, we performed both object- and pixel-based classification using the SVM algorithm. Three iterations were performed: the first one with the 8 classes listed in Tab.1; the second iteration with 7 classes as Asphalt and Urban were merged; the third one with 6 classes as Industrial was merged too. Tables 4 to 7 show the confusion matrix for object- and pixel-based classification, for iteration 1 and 2; the third iteration is not illustrated since it gave limited improvements.

Table 4: Confusion matrix for the first object-based classification.

Object-based		Reference Dataset								Classified Totals	UA
		Bare soil	Urban	Industrial	Asphalt	Water	Grassland	Wood	Barley		
Classified Data	Bare soil	2552	33	10	13	16	34	2	8	2668	0.957
	Urban	250	366	13	20	0	2	0	0	651	0.562
	Industrial	1	0	46	0	0	0	0	0	47	0.979
	Asphalt	0	0	0	12	0	0	1	0	13	0.923
	Water	0	0	0	0	68	0	0	0	68	1.000
	Grassland	2	0	0	0	0	430	16	21	469	0.917
	Wood	73	0	1	1	0	25	633	36	769	0.823
	Barley	21	0	0	0	5	57	64	170	317	0.536
Reference Totals		2899	399	70	46	89	548	716	235	5002	
PA		0.880	0.917	0.657	0.261	0.764	0.785	0.884	0.723	OA	0.855
										Kappa	0.775

Table 5: Confusion matrix for the first pixel-based classification.

Pixel-based		Reference Dataset								Classified Totals	UA
		Bare soil	Urban	Industrial	Asphalt	Water	Grassland	Wood	Barley		
Classified Data	Bare soil	2514	72	26	13	4	29	23	30	2711	0.927
	Urban	276	312	6	14	0	4	0	0	612	0.510
	Industrial	2	9	38	3	0	0	0	0	52	0.731
	Asphalt	4	4	0	15	0	0	1	1	25	0.600
	Water	0	0	0	0	85	0	0	0	85	1.000
	Grassland	40	1	0	0	0	452	7	38	538	0.840
	Wood	25	1	0	0	0	22	640	19	707	0.905
	Barley	38	0	0	1	0	41	45	147	272	0.540
Reference Totals		2899	399	70	46	89	548	716	235	5002	
PA		0.867	0.782	0.543	0.326	0.955	0.825	0.894	0.626	OA	0.840
										Kappa	0.751

Table 6: Confusion matrix for the second object-based classification.

Pixel-based		Reference Dataset							Classified Totals	UA
		Bare soil	Industrial	Water	Grassland	Wood	Barley	Asphalt+ Urban		
Classified Data	Bare soil	2538	24	7	27	20	36	97	2749	0.923
	Industrial	9	39	0	0	0	0	19	67	0.582
	Water	2	0	82	0	0	1	0	85	0.965
	Grassland	51	0	0	453	2	28	0	534	0.848
	Wood	23	0	0	15	648	22	2	710	0.913
	Barley	19	0	0	50	45	148	0	262	0.565
	Asphalt+Urban	257	7	0	3	1	0	326	594	0.549
Reference Totals		2899	70	89	548	716	235	444	5001	
PA		0.875	0.557	0.921	0.827	0.905	0.630	0.734	OA	0.847
									Kappa	0.759

Table 7: Confusion matrix for the second pixel-based classification.

Object-based		Reference Dataset							Classified Totals	UA
		Bare soil	Industrial	Water	Grassland	Wood	Barley	Asphalt+ Urban		
Classified Data	Bare soil	2380	2	39	42	21	3	151	2638	0.902
	Industrial	8	117	0	0	0	0	19	144	0.813
	Water	0	0	70	0	0	0	0	70	1.000
	Grassland	5	0	0	462	9	3	0	479	0.965
	Wood	43	0	16	35	620	10	3	727	0.853
	Barley	40	0	0	16	36	255	1	348	0.733
	Asphalt+Urban	151	17	0	1	42	0	383	594	0.645
Reference Totals		2627	136	125	556	728	271	557	5000	
PA		0.906	0.860	0.560	0.831	0.852	0.941	0.688	OA	0.857
									Kappa	0.788

Concerning the first iteration, the two methods achieved a satisfactory overall accuracy and a very good Kappa coefficient, presenting minimal differences. However, by analyzing the confusion matrix in detail, we observed errors.

In relation to the object-based classification (Table 4), the lower PA is that of Asphalt with a value of 26%. The Asphalt class was often confused with that of the Urban. We did not observe the opposite error,

i.e. Urban was never classified as Asphalt. In addition, the Industrial class was classified as Urban in 13 cases out of 70, resulting in a PA of 66%. Also, in this case, the opposite error was never observed, i.e. Urban was never classified as Industrial. As concerning the UA, we have low values for the Urban, which was classified as Bare Soil (250 out of 651), as we can see in Table 4. Similarly, in the pixel-based confusion matrix (Table 5), it was possible to observe confusion between Urban and Asphalt categories (although slightly less frequent) and classification errors between Bare soil and Urban classes (a little more frequent). The distinction between Urban, Industrial and Asphalt classes is not a major requirement in view of our future project of crop detection. As already mentioned, given the described classification errors, it was decided to perform a second iteration after merging the Urban and Asphalt classes and a third one by aggregating Industrial too. Such strategy aimed at improving accuracy without losing discrimination power between agricultural crops.

A third iteration did not achieve a substantial improvement, and therefore results from the second one (characterized by the merge of Asphalt and Urban into a unique category) are briefly discussed.

By observing the confusion matrix derived from the second iteration of the object-based classification (Table 6), and comparing it with that corresponding to the first iteration, it was immediately observed that all the PA values were greater than 0.5 and those of the UA were greater than 0.6. In particular, for the Asphalt class the low PA of 0.26 did not appear. The same observation can be applied to the second iteration of pixel-based classification matrix (Table 7), compared with the corresponding matrix of the first iteration. The PA values were always higher than 0.55, whereas the UA was always higher than 0.54. In particular, for the Asphalt class the low PA of 0.33 did not appear. On the other hand, a reduction of the PA and UA accuracy of some classes, for example the PA of Water in the object-based matrix, was found. Essentially, there were fewer accuracy problems with the pixel-based classification.

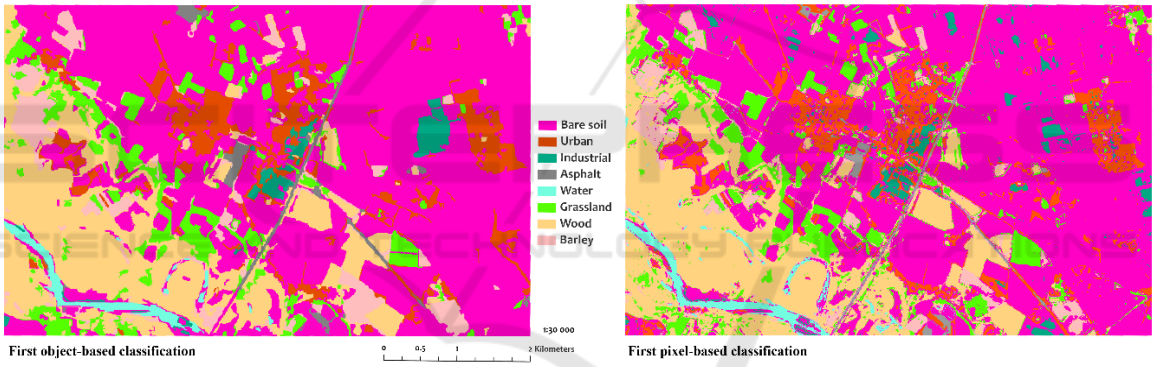

Figure 5: Land cover maps resulting from the first iteration. On the left: Object-based classification. On the right: Pixel-based classification.

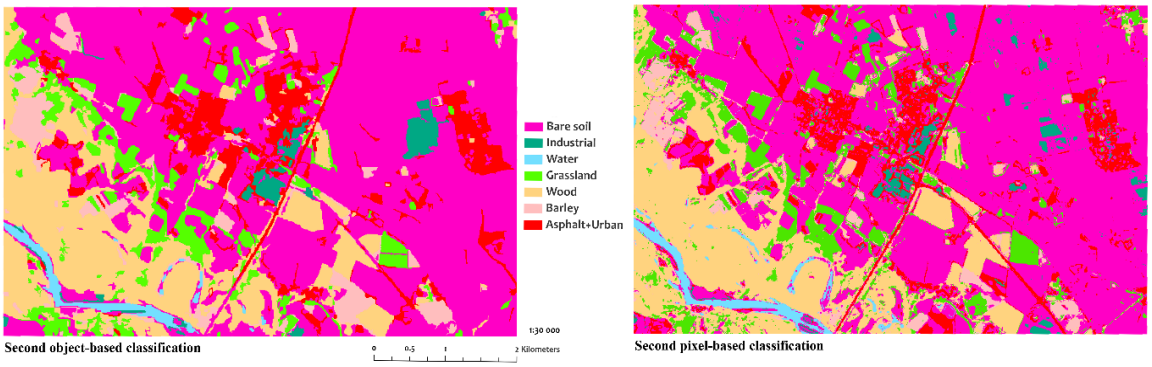

Figure 6: Land cover maps resulting from the second iteration, after merging Asphalt and Urban (seven land cover types). On the left: Object-based classification. On the right. Pixel-based classification.

The direct comparison between the two matrices of the second iteration shows that the object-based classification is more suitable for the Industrial class and for the Barley class, while the pixel-based classification better predicts Water. Naturally, the improvement of both compared to the first level is due precisely to the incorporation of classes Asphalt and Urban. It can be said that, in general, the pixel-based method offers a higher average performance than the object-based, unless a specific class is only focused.

Table 8: Overall Accuracy Summary of the first and second iteration.

	I object-based	I pixel-based	II object-based	II pixel-based
OA	0.855	0.840	0.857	0.846

Land cover maps for both methodologies and iterations 1 and 2 are shown in Figures 5, 6.

A final remark concerns processing time. Object-based classification takes a few minutes for segmentation on a quad-code personal computer and another few minutes for training and classification. Pixel-based needs several hours.

5 CONCLUSIONS

The workflow presented in this study was developed with the aim of evaluating the potentials obtainable from the classification of remote sensing images provided by the Sentinel-2 satellites, in particular that of creating land covers and use maps. The study area concerned a neighboring area to the town of Pavia, Italy. Data for training and accuracy assessment was personally collected by interviewing farm owners, observing a very high-resolution satellite image and with inspection of the areas pertained to as well. The date May 17th 2017 was chosen for the study.

As inputs, 10 spectral bands resampled to 10 m were used. Through ArcGIS Pro (Esri), the pixel-based and object-based supervised classifications were applied, using the multiclass SVM algorithm. The procedures were iterative, to best satisfy the levels of accuracy desired. Thanks to the different bands available that allow recognizing specific spectral signatures for the objects observed, the multispectral image used has been well suited to the identification of the different types of coverage present in the area of interest. It can be said that in general the pixel-based method offers a better average performance than the object-based one, unless interested in specific classes. However, the two methods offer a comparable overall accuracy. On the other hand, it is also necessary to take into account the processing time: a few minutes in the case of object-based classification, several hours for the pixel-based method. Considering the overall accuracy results obtained in this study (Table 8), we can conclude that the supervised method is quite effective for land cover detection.

REFERENCES

Abdi, H., Williams, L. J., 2010. Principal component analysis. In *Wiley Interdisciplinary Reviews: Computational Statistics, vol. 2, no. 4, pp. 433-459.*

Chhetri, N., Chaudhary, P., Tiwari, P. R., Yadaw, R. B., 2012. Institutional and technological innovation: Understanding agricultural adaptation to climate change in Nepal. *Applied Geography, 33*, 142-150.

Comaniciu, D., Meer, P., 2002. Mean shift: A robust approach toward feature space analysis. *IEEE Trans. Pattern Anal. Mach*. Intell. , 24, 603–619.

DESA, U., 2017. World population prospects, the 2017 *Revision, Volume I: comprehensive tables*. New York United Nations Department of Economic & Social Affairs.

Fukunaga, K., Hostetler, L., 1975. The estimation of the gradient of a density function, with applications in pattern recognition. *IEEE Trans. Inf. Theory*, 21, 32–40.

Immitzer, M., Vuolo, F., Atzberger, C., 2016. First Experience with Sentinel-2 Data for Crop and Tree Species Classifications in Central Europe, *Remote Sensing.*

Kowalczyk, A., 2017. *Support Vector Machines succinctly*, Succinctly E-book series, Syncfusion Inc.

Marais-Sicre, C., Inglada, J., Fieuzal, R., Baup, F., Valero, S., Cros, J., Huc, M., Demarez, V., 2016. Early Detection of Summer Crops Using High Spatial Resolution Optical Image Time Series, *Remote Sensing.*

MiPAAF, 2017. Linee Guida per lo Sviluppo dell'Agricoltura di precisione in Italia. In *Pubblicazioni Ministero delle Politiche Agricole Alimentari e Forestali*

Pierce, F. J., Nowak, P., 1999. Aspects of precision agriculture. In *Advances in agronomy.*

Schwartz, M. D., 2003. *Phenology: An Integrative Environmental Science*, Dordrecht: Kluwer Academic Publishers.

Taskin Kaya, G., Musaoglu, N., Ersoy, O. K., 2011. Damage assessment of 2010 Haiti earthquake with post-earthquake satellite image by support vector selection and adaptation. *Photogrammetric Engineering & Remote Sensing*, 77(10), 1025-1035.

URL-1: http://www.geoportale.regione.lombardia.it

Vapnik, V., 1979. Estimation of Dependences Based on Empirical Data. Nauka, Moscow, pp. 5165–5184, 27 (in Russian) (English translation: Springer Verlag, New York, 1982).

Zarco-Tejada, P., Hubbard, N., Loudjani, P., 2014. Precision Agriculture: An Opportunity for EU Farmers - Potential Support with the CAP 2014-2020. In *Joint Research Centre (JRC) of the European Commission publication*